The Distribution of Grain Boundary Planes in Polycrystals

Gregory S. Rohrer

During the last ten years, techniques have been developed to measure the distribution of grain boundaries in polycrystals as a function of both lattice misorientation and grain boundary plane orientation. This paper presents a brief overview of the techniques used for these measurements and the principle findings of studies implementing these techniques. The most significant findings are that grain boundary plane distributions are anisotropic, that they are scale invariant during normal grain growth, that the most common grain boundary planes are those with low surface energies, that the grain boundary populations are inversely correlated with the grain boundary energy, and that the coincident site lattice number is a poor predictor of the grain boundary energy and population.

INTRODUCTION

The structural characterization of polycrystalline solids has historically included quantitative metrics such as the mean grain size and grain size distribution, the grain shape, the grain orientation texture, and the misorientation texture. More recently, it has become possible to measure the distribution of interface plane orientations.[1,2] For the case of single-phase polycrystals, the grain boundary plane orientation distribution is specified by the five parameter grain boundary character distribution (GBCD). The GBCD is defined as the relative areas of grain boundaries of different types, distinguished by their lattice misorientation and grain boundary plane orientation. To illustrate how the five parameter description of grain boundar-

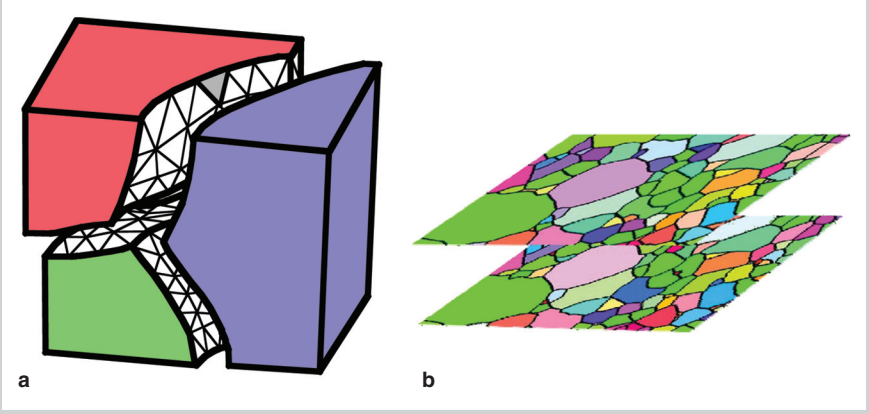

Figure 1. (a) A representation of a three-grain junction within a polycrystal. The view is exploded so that the internal interfaces can be seen. The external surfaces are shaded and the internal surfaces are triangulated to indicate grain boundaries with distinct orientations. (b) An oblique view of two parallel orientation maps on sequential serial sections of a polycrystal. Each color corresponds to a unique grain orientation and the black lines represent grain boundaries.

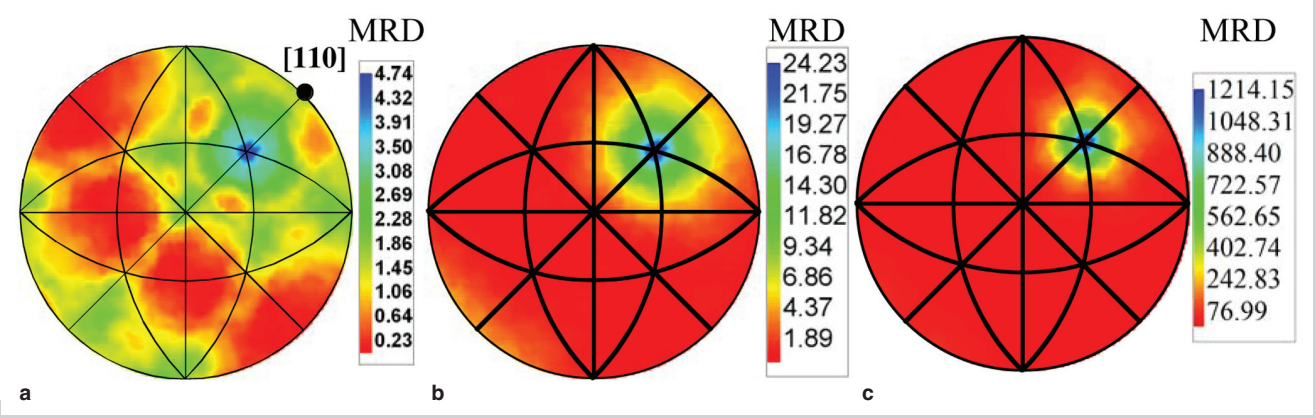

Figure 2. Grain boundary plane distributions for the Σ3 misorientation (this is a misorientation of 60° around [111]) in (a) MgO, (b) aluminum, and (c) nickel. In each case, the distribution peaks at the orientation of the (111) plane, indicating that most of the grain boundaries are perpendicular to the misorientation axis.

ies differs from simpler parameterizations, consider the schematic in Figure 1a, where the interfaces between three grains are illustrated. Distinguished by lattice misorientation, there are three distinct grain boundaries separating the three crystals. However, in the five parameter description, the interfacial surfaces are broken up into planar units of distinct orientation so that each of the individual triangles that make up the interfacial surfaces corresponds to different types of grain boundaries.

It is obvious that this parameterization greatly increases the number of distinguishable grain boundary types relative to parameterizations based only on lattice misorientation (three parameters) or the disorientation angle (one parameter). Consider the case of a polycrystal with cubic symmetry and assume that the angular parameters are distinguished with 10° of resolution. Using the one-parameter description there are six distinct boundaries, using the three-parameter description there are about 25 distinct boundaries, and using the five-parameter description there are approximately 6.5×10^3 distinct boundaries.[1] While the additional parameters increase the complexity of characterizing the structure, they are also very important because it is well known that grain boundary properties vary significantly with grain boundary plane orientation. For example, the mobility and energy of Σ3 grain boundaries in cubic materials (the grain boundary formed by a 60° rotation about a mutual <111> axis) vary strongly with the orientation of the grain boundary plane; the minimum energy and mobility are found at the coherent twin configuration where both crystals are terminated at the boundary by {111} planes.[3,4]

Examples of the grain boundary plane distributions for the Σ3 grain boundary in MgO, aluminum, and nickel are shown in Figure 2. The distributions are plotted on stereographic projections measured in multiples of a random distribution (MRD) such that values greater than unity signify grain boundary types that are observed more frequently than expected. All three distributions peak at the position of the pure twist configuration, where the grain boundary plane is perpendicular to the misorientation axis; this is the position of the coherent twin.

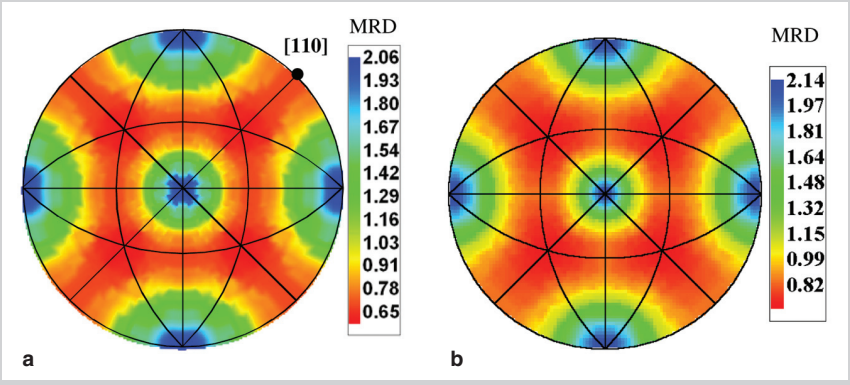

Figure 3. Grain boundary plane distribution (independent of misorientation) for two MgO samples with different grain sizes. (a) Grain size = 24 μm, (b) grain size = 100 μm. The small differences in the distributions are within the limits of experimental uncertainties.

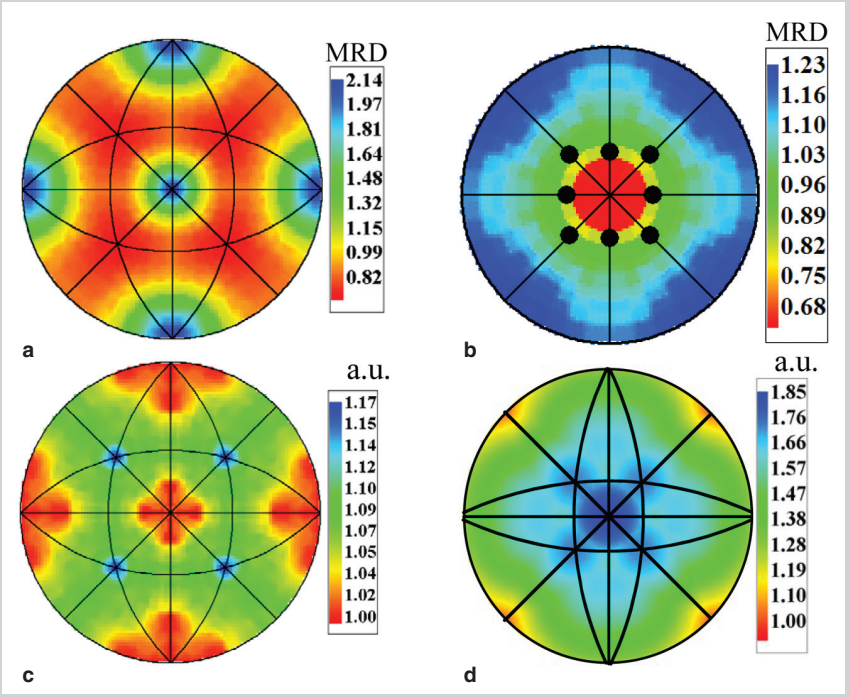

Figure 4. A comparison of measured grain boundary plane distributions in MgO (cubic) and TiO_2 (tetragonal) with the measured surface energies in the same materials. (a) The grain boundary plane distribution of MgO.[30] (b) The measured surface energy of the same sample.[29] (c) The grain boundary plane distribution of TiO_2. (d) The measured surface energy of the same sample.[19]

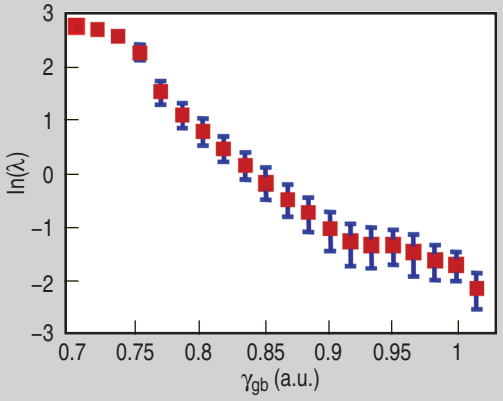

Figure 5. The logarithm of the grain boundary population (λ) in MgO as a function of the grain boundary energy (γ_{gb}). The mean is represented by the point; the bars indicate one standard deviation. The graph is constructed based on the data in Reference 32.

Note that the three materials exhibit different degrees of anisotropy and the intensity of the peak at the coherent twin orientation is inversely related to the stacking fault energy.

The challenge of measuring the five-parameter GBCD is that a large number of observations must be made to sample the entire space of grain boundary types. This challenge has largely been met by computer-automated measurements that allow statistical information on hundreds of thousands of grain boundaries to be collected in a time period on the order of a few days.

MEASURING THE DISTRIBUTIONS OF INTERFACE ORIENTATIONS

Measurements of the crystallography of interface planes are currently based on electron-backscatter diffraction (EBSD) mapping in the scanning-electron microscope (SEM).[5] The SEM is used to produce backscatter diffraction patterns that are digitally captured and automatically indexed to determine the crystallographic orientation of the diffracting volume. When this process is repeated at a sequence of predetermined locations, orientation maps can be recorded. Grains are identified as areas of constant orientation and grain boundaries are defined as the positions where there is an abrupt change in orientation (see Figure 1b). Based on such orientation maps, the lattice misorientation across any grain boundary can be specified as well as the zone axis of the grain boundary plane. In other words, four of the five parameters needed to specify the grain boundary character distribution are known. There are two approaches to determining the inclination of the grain boundary with respect to the sample section plane: serial sectioning and stereology.

Serial sectioning refers to the process in which multiple parallel planar sections are used to reconstruct the three-dimensional (3-D) grain boundary network. As an example, two orientation maps from sequential serial sections are shown in Figure 1b. Sectioning can be accomplished by conventional polishing or milling, or it can be accomplished by ion beam milling in a dual beam-focused ion beam (DB-FIB) SEM. There are several important requirements that must be met

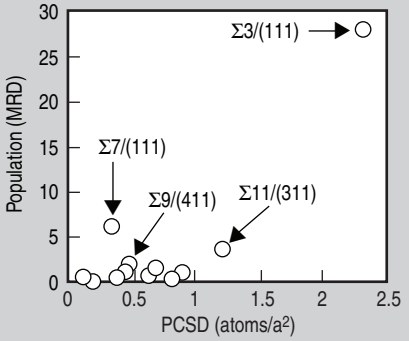

Figure 6. The population of grain boundaries in aluminum versus the planar coincident site density (PCSD) for the 13 symmetric grain boundaries with $\Sigma \leq 11$.[22] The four highest population boundaries are labeled; there is no obvious correlation between the population and the PCSD.

for an accurate reconstruction. The first is that the amount of material removed between the section planes must be small in comparison to the grain size. The second is that it must be possible to align and position the images of each section plane in 3-D space. Finally, the line segments that come from the same interface, but appear on different sections, must be identified and connected.

Serial sectioning using conventional polishing[6–8] or milling machines[9,10] can remove material with thicknesses on the order of a few micrometers while the focused ion beam can remove layers with thicknesses that are a fraction of a micrometer.[11,12] Alignment of the sections is usually accomplished using fiducial marks, and the most common are intentionally induced marks from a Vickers hardness indenter.[13] Since the indenter tip leaves marks of known shape, both the alignment of the layers and the vertical position can be determined. If the grains do not have a shape anisotropy, then alignment of large areas can be accomplished using the grains[6] or triple junctions[14] as the fiducial marks. In this procedure, the relative position of each layer is determined by assuming that the positions of the microstructural features (the centers of grains or triple junctions) are randomly distributed about the sample normal. When EBSD data is available, it is also possible to position adjacent layers based on the relative disorientation between voxels in adjacent layers.[15]

Since the indenter tip leaves marks of known shape, both the alignment of the layers and the vertical position can be determined.

The GBCD can also be determined stereologically from observations on a single section plane.[16] However, it should be kept in mind that the stereological method does not provide detailed information on specific boundaries, but instead provides information on the distribution of boundary types. The complete method is described in detail in Reference 16. Briefly, by observing many grain boundary traces from crystallographically indistinguishable bicrystals in different relative orientations with respect to the viewing plane, it is possible to determine the true distribution of grain boundary planes. There are several requirements that must be met to use this method. The first is that one needs a sufficient number of observations. This has been estimated to be roughly 2,000 grain boundary line segments on a single section plane for each distinguishable misorientation type.[16] The second is that the grain boundary trace positions must be determined with sufficient accuracy. In practice, the spacing between the EBSD orientation pixels should be no larger than one tenth the average grain diameter. Finally, the traces must be sampled from randomly oriented bicrystals. In other words, if the sample has significant grain orientation texture, it will bias the result. Fortunately, this is a practical rather than fundamental limitation and it is expected that techniques for the stereological analysis of the GBCD from textured specimens with be developed in the near future.

OBSERVED PROPERTIES OF THE GBCD

Grain Boundary Pane Distributions are Anisotropic

In studies of a wide range of ceramic and metallic polycrystals, including MgO,[6] $SrTiO_3$,[17] $MgAl_2O_4$,[18] TiO_2,[19] WC,[20,21] Al,[22] Cu,[23] Ni,[24] α-brass,[25] and stainless steel,[26] the authors have found

that grain boundary plane distributions have significant anisotropy at fixed misorientations (for example, see Figure 2). Even in relatively isotropic materials, such as aluminum, there are many peaks that exceed 3.0 MRD.[22] The favored grain boundary planes typically correspond to low index orientations. It is also noteworthy that grain boundaries that occur at the peaks in the distribution have greater number densities and larger average areas than other types of grain boundaries.[17]

The Grain Boundary Character Distribution is Scale Invariant

Simulations of capillary-driven grain growth with anisotropic grain boundary properties have indicated that the five-parameter GBCD reaches a steady state that is not affected by further grain growth.[27] This is consistent with experimental data, such as that shown in Figure 3. When the grain size increases by a factor of 4, approximately one in 4,000 of the initial grains remain and the vast majority of the initial interfacial areas are eliminated. The consistency of the GBCD throughout this process indicates that the factors determining the populations are highly deterministic.

The Most Common Grain Boundary Planes are Those with Low Surface Energies

The distribution of grain boundary planes (averaged over misorientation) always exhibits peaks at the positions of the low-index, low-surface-energy planes.[28] This is illustrated in Figure 4, where the grain boundary plane distributions and measured surface energies for MgO and TiO_2 are compared.[19,29,30] In both cases, the surface energy reaches a minimum at the orientations where the grain boundary plane distribution reaches a maximum. The predominance of internal planes with low surface energy suggests that the grain boundaries made up of these planes also have a low energy. The grain boundary energy must be equal to the sum of the energies of the two free surfaces on either side of the boundary, minus a binding energy that arises from the bonds formed when the two surfaces are brought together.[31] Thus, these observations suggest that variations in the binding energy are small compared to the variations in the surface energy.

Grain Boundary Populations are Inversely Correlated with the Grain Boundary Energy

The implication of the observation discussed above is that the grain boundaries with low energy are favored in the distribution. While grain boundary energy data is more scarce than surface energy data, one comprehensive set of measured grain boundary energies exists and has been compared to the GBCD of the same material.[32] The result illustrated in Figure 5 clearly shows the low-energy grain boundaries are represented more frequently in the distribution than high-energy grain boundaries and that the logarithm of the population exhibits an approximate inverse linear relationship with the energy. This suggests that deterministic, energy-driven mechanisms are operative in developing the GBCD and a mechanistic theory for the development of the GBCD has recently been proposed.[33]

Coincident Site Lattice Number is a Poor Predictor for Grain Boundary Energy or Population

The coincident site lattice (CSL) concept has been in use for more than 50 years.[34] The basic idea is that boundaries with misorientations that place a high fraction of lattice sites in coincidence are distinguished from more general boundaries. These CSL boundaries are assigned a coincidence number (Σ) based on the inverse of the number of coincident lattice sites.[35] Therefore, a low Σ number signifies high coincidence. It seems intuitive that boundaries between grains whose lattices exhibit partial coincidence would have lower energies and distinct properties. However, lattice coincidence is likely to have physical significance only when it occurs in the boundary plane and, even when this is taken into account, an analysis of the grain boundary plane distributions at low Σ CSL misorientations in several materials indicated that the coincidence concept is a poor predictor of grain boundary energy and population.[36] This is illustrated in Figure 6, which compares the planar coincident site density for grain boundaries in aluminum with their populations.[22] Although it is notable that the coherent twin has both the highest coincidence and greatest population, the remainder of the data exhibit no correlation. In a comparison of four different materials, the distributions of grain boundary planes at misorientations with high lattice coincidence were not found to be substantially different from the distributions at other, more general misorientations.[36] Further, in most situations, the most frequently adopted grain boundary orientation is a habit plane of low index and low surface energy that depends on the particular material.[36] The results indicate that a model for grain boundary energy and structure based on grain surface relationships is more appropriate than the widely accepted models based on lattice orientation relationships.

CONCLUSION

Grain boundary plane distributions in polycrystals are anisotropic and scale invariant during normal grain growth. This suggests that the GBCD is an intrinsic characteristic of the microstructure. The most common grain boundary planes are those with low surface energies and the grain boundary populations are inversely correlated with the grain boundary energy. These observations indicate that the GBCD develops deterministically based on the relative energies of the boundaries and can be influenced by altering these energies. Finally, results suggest that the coincident site lattice number and the planar coincident site density are poor predictors for the grain boundary energy and population.

ACKNOWLEDGEMENT

This work was supported primarily by the Materials Research Science and Engineering Centers (MRSEC) program of the National Science Foundation under Award Number DMR-0520425. The author acknowledges the contributions of his many colleagues in the Carnegie Mellon University MRSEC, including Herb Miller, Jason Gruber, David Saylor, Chang-Soo Kim, Sukbin Lee, Francine Papillon, Paul Wynblatt, and Tony Rollett.

References

1. G.S. Rohrer et al., *Z. Metal.,* 95 (2004), pp. 197–214.
2. C.-S. Kim, A.D. Rollett, and G.S. Rohrer, *Scripta Mater.*, 54 (2006), pp. 1005–1009.
3. U. Wolf et al., *Phil Mag A,* 66 (1992), pp. 991–1016.

4. K.G.F. Janssens et al., *Nature Materials*, 5 (2006), pp. 124–127.
5. B.L. Adams, S.I. Wright, and K. Kunze, *Met. Trans.*, 24A (1993), pp. 819–831.
6. D.M. Saylor, A. Morawiec, and G.S. Rohrer, *Acta Mater.*, 51 (2003), pp. 3663–3674.
7. M. Lanzagorta et al., *Ninth IEEE Visualization, VIS'98* (1998), pp. 487–490.
8. V. Randle and H. Davies, *Ultramicroscopy*, 90 (2002), pp. 153–162.
9. J. Alkemper and P.W. Voorhees, *Acta Mater.*, 49 (2001), pp. 897–902.
10. J. Alkemper and P.W. Voorhees, *J. Microscopy*, 201 (2001), pp. 388–394.
11. M.D. Uchic et al., *Scripta Mater.,* 55 (2006), pp. 23–28.
12. D.J. Rowenhorst et al., *Scripta Mater.,* 55 (2006), pp. 11–16.
13. V. Randle and O. Engler, *Introduction to Texture Analysis: Macrotexture, Microtexture, & Orientation Mapping* (Amsterdam: Gordon and Breach Science Publishers, 2000).
14. A. Morawiec and D. Saylor, *Proceedings of ICOTOM-12,* ed. J. Szpunar (Ottawa, Canada: NRC Research Press, 1999), pp. 198–203.
15. S.-B. Lee, A.D. Rollett, and G.S. Rohrer, *Materials Science Forum,* 558-559 (2007), pp. 915–920.
16. D.M. Saylor et al., *Metallurgical and Materials Transactions*, 35A (2004), pp. 1981–1989.
17. D.M. Saylor et al., *J. Amer. Ceram. Soc.*, 87 (2004), pp. 670–676.
18. H.M. Miller et al., *Materials Science Forum*, 467-470 (2004), pp. 783–788.
19. Y. Pang and P. Wynblatt, *J. Am. Ceram. Soc.*, 89 (2006), pp. 666–671.
20. C.-S. Kim and G.S. Rohrer, *Interface Science*, 12 (2004), pp. 19–27.
21. C.-S. Kim (Ph.D. thesis, Carnegie Mellon University, 2004).
22. D.M. Saylor et al., *Acta Mater.*, 52 (2004), pp. 3649–3655.
23. V. Randle, G. Rohrer, and G. Owen, *Anisotropy, Texture, Dislocations, and Multiscale Modeling in Finite Plasticity and Viscoplasticity and Metal Forming*, ed. A.S. Khan and R. Kazmi (Publisher's Location: Neat Press, Inc., 2006), p. 307.
24. H.M. Miller et al., *Materials Science Forum*, 558-559 (2007), pp. 641–647.
25. G.S. Rohrer et al., *Acta Mater.*, 54 (2006), pp. 4389–4502.
26. S. Downey II et al., *J. Mater. Sci.*, in press.
27. J. Gruber et al., *Scripta Mater.*, 53 (2005), pp. 351–355.
28. D.M. Saylor et al., *J. Amer. Ceram. Soc.*, 87 (2004), pp. 724–726.
29. D.M. Saylor and G.S. Rohrer, *Interface Science*, 9 (2001), pp. 35–42.
30. D.M. Saylor, A. Morawiec, and G.S. Rohrer, *J. Amer. Ceram. Soc.*, 85 (2002), pp. 3081–3083.
31. D. Wolf, *J. Mater. Res.*, 5 (1990), pp. 1708–1730.
32. D.M. Saylor, A. Morawiec, and G.S. Rohrer, *Acta Mater.*, 51 (2003), pp. 3675–3686.
33. G.S. Rohrer, J. Gruber, and A.D. Rollett, *Scripta Mater.*, submitted.
34. M.L. Kronberg and F.H. Wilson, *Met. Trans.*, 185 (1949), pp. 501–514.
35. H. Grimmer, W. Bollmann, and D.H. Warrington, *Acta Cryst.*, A30 (1974), pp. 197–207.
36. G.S. Rohrer et al., *Mat. Res. Soc. Symp. Proc.*, 819 (Warrendale, PA: Materials Research Society, 2004), N7.2.

Gregory S. Rohrer is with the Department of Materials Science and Engineering, Carnegie Mellon University, Pittsburgh PA, 15213 and can be reached at gr20@andrew.cmu.edu.

Your Partner in Materials Analysis

Experienced analysis with a wide variety of materials including:

- Metals
- Polymers
- Composites
- Refractory materials
- Ceramics

Visit us at MS&T '07 Booth 331 September 16-20 Detroit, MI

Specialized Testing Capabilities

- Elemental and Chemical Analysis
- SEM/EDS
- Microscopy
- Thermal Analysis
- Surface Analysis

NSL ANALYTICAL
www.nslanalytical.com

NSL Analytical Services, Inc.
4450 Cranwood Parkway, Cleveland, Ohio 44128
Toll Free: 800.497.6752 • nsl@nslanalytical.com
Nadcap and ISO/IEC 17025 Accredited

Trust | Technology | Turnaround

Read *JOM* On-Line . . . Just Like You Do in Print!

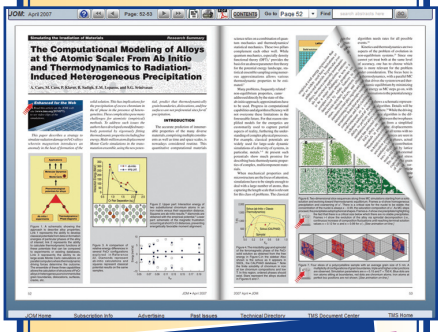

Now featuring *JOM Extra*, an online-only supplement of commercial process and product news.

Turn the Pages, Click the Links at: *http://www.tms.org/JOMPT*